Electron Microscopy and Diffraction of Layered, Superconducting Intercalation Complexes

Abstract. *Several layered, transition metal dichalcogenide intercalation complexes with unique superconducting properties have been examined by high-resolution electron microscopy and electron diffraction. Details of the crystalline lattice and of the lattice imperfections have been directly resolved. The results can be correlated with the available x-ray diffraction and chemical data, and they confirm and extend the postulated models.*

Gamble and his colleagues (*1–3*) have recently described a new class of layered transition metal dichalcogenide intercalation complexes with unique superconducting properties [see also (*4*)]. These exceptionally anisotropic, crystalline, metallic complexes are bulk superconductors which may have useful high magnetic field properties.

The unusual features of these superconductors and the available data on their composition provided favorable conditions for further elucidation of their structure by electron microscopy. Correlated high-resolution electron microscopy and electron diffraction investigations have been carried out on representative samples of these new compounds supplied by Gamble and his colleagues. Improved high-voltage instrumentation and preparation techniques were required to resolve significant details of the atomic lattice in microcrystalline specimens of the complexes. We report here on the results of these studies which have permitted the first direct visualization of the layered structure of the metallic superconductors TaS_2 and selected $TaS_2(C_5H_5N)$ intercalation complexes.

It has also been possible to make precision determinations of the basic lattice parameters of the minute single crystals by correlating the electron microscope images with the corresponding selected-area electron diffraction patterns. The extraordinary regularity of the metallic layers disposed in parallel arrays and the distinctive interlayer structures revealed in certain regions of these crystalline complexes by electron microscopy confirm and extend the postulated models (*1, 2*). In addition, numerous dislocations and other types of intrinsic lattice imperfections have now been recognized as characteristic features which may bear on the unique superconducting properties of these crystals.

Powders and crystals of 2H-TaS_2 and of the intercalation complexes $TaS_2(C_5H_5N)_{1/2}$ and $TaS_2(C_5H_5N)_{1/4}$ prepared by Gamble *et al.* (*1, 2*) were examined under clean room conditions in a controlled environment. The microcrystalline specimens cleave readily, and, unlike hard crystals, they can be prepared as ultrathin layers without the introduction of visible deformations. The lamellae were picked up directly on ultrathin carbon films or on special fenestrated substrates (*5*), and precautions were taken to avoid water or solvent contamination. The specimens were examined by high-resolution electron microscopy with a centrally regulated power supply for the modified microscopes which operate at 75 and 100 kv and are provided with objective lenses with short focal lengths. Radiation damage and specimen contamination were reduced by the use of microbeam illumination and cooling devices operated at liquid-nitrogen temperatures.

Most of the studies were carried out with a 200-kv high-voltage HU-200E electron microscope, which has demonstrated greater penetration power, increased diffraction accuracy, and reduced radiation damage in specimens approximately 100 to 600 Å thick. Resolutions of 2 to 3 Å were consistently achieved in all microscopes used under optimum conditions (*6, 7*) for the direct imaging of the atomic lattice and related structural details. We determined the crystalline lattice parameters by rapidly recording sequential electron diffraction patterns of suitable areas (about 1 μm^2) from the imaged specimen field, and then by carefully processing the photographic emulsions to ensure reproducible conditions for precision measurements with a special comparator. By comparing the electron diffraction patterns with patterns from the standard specimen [a single-crystal gold film, (200) plane orientation with a spacing of 2.04 Å] recorded under identical conditions, and by repeated measurements with a precision comparator, we were able to determine the average lattice spacings in the layered crystalline specimens with a probable error of 0.005 Å. These lattice values are in reasonable agreement with the available x-ray powder diffraction data (*2*) derived from a polycrystalline aggregate composed of millions of atomic planes, whereas the electron diffraction data refer directly to a microscopic specimen region less than 100 atomic layers thick. The results we report here are based on detailed evaluation of 4000 electron micrographs and diffraction patterns.

These layered crystals are ideal specimens for high-resolution electron microscopy because they can be cleaved into ultrathin layers which display a periodic lattice with heavy metal atoms incorporated in repetitive patterns, thus contributing to the enhancement of phase and diffraction contrast for visualization of the original atomic distribution. Improved instrumentation combined with these factors probably accounts for the direct imaging of the atomic lattice in suitably oriented crystalline lamellae (Fig. 1A) or in thin microcrystals precisely aligned with their layers parallel to the incident electron microbeam (Fig. 1B). The multilayered spacing with a periodicity of 6 Å observed in the 2H-TaS_2 specimens can be correlated with the 6.052-Å reflection recorded in the selected-area electron diffraction pattern which corresponds to the metallic crystalline layer spacing and is in good agreement with the equivalent spacing of 6.05 Å derived from the x-ray powder diagram of the bulk specimen (*2, 8*).

When the incident electron beam is normal to the *a* plane in thin TaS_2 crystals, regular hexagonal moiré patterns are seen as transmission images of overlapping layers of TaS_2 planes which represent indirect resolution of the atomic array at the level of 1 Å or less (*9*). This spacing is particularly relevant to the study of lattice imperfections.

The 2H-$TaS_2(C_5H_5N)_{1/2}$ compound is a highly crystalline, stoichiometric complex characterized on the basis of x-ray powder diffraction patterns as indexable on a hexagonal unit cell with two layers of TaS_2 per cell ($a = 3.315$ Å and $c/2 = 12.02$ or 11.85 Å). Two molecular stacking arrangements ($c/2 = 12.02$ or 11.85 Å) apparently occur in these compounds (*2*).

Electron microscopy of the ultrathin crystalline lamellae reveals a regular arrangement of dense layers separated by less dense layers (Fig. 1b), which generally feature a faint intermediate line. A particularly well-oriented crystallite yielded the single-crystal electron diffraction pattern shown in Fig. 1C. The large number of highly ordered reflections permitted accurate determi-

nation of the lattice parameters. The (001) reflections correspond to the layer spacing of 12.001 Å, and the calculated a axis parameter is 3.335 ± 0.005 Å. These values and the slightly lower layer spacings of 11.847 Å found in other specimens are in agreement with the corresponding x-ray diffraction data reported by Gamble *et al.* (*1, 2*).

Specimens of the fairly pure second-stage complex, $TaS_2(C_5H_5N)_{1/4}$, in which two layers of TaS_2 are separated by intercalated pyridine, reveal a distinctive pattern of two dense lines separated by a uniform light layer to give a repeating period of 18 Å in the electron micrographs (Fig. 1D), corresponding to an average value of 17.639 Å in the selected-area electron diffraction patterns. This layer spacing is in agreement with the corresponding x-ray diffraction spacing [see (*4*)]. As shown in Fig. 1D, the faint intermediate line is regularly seen in the central region of the light layer. In both $TaS_2(C_5H_5N)_{1/4}$ and $TaS_2(C_5H_5N)_{1/2}$ complexes, this uniform light layer is approximately 8 to 10 Å thick and thus represents a major component of the periodic layered structure. These dimensions and the intermediate line found in the central region of the light layer must be taken into account, since all of the available evidence suggests that this line and the light layer are related to the relatively electron-transparent intercalated pyridine molecules which separate the electron-dense TaS_2 layers in these organometallic compounds. Further work is required to determine the orientation of the pyridine molecules. The slight increases in the a axis on intercalation, as confirmed by x-ray and electron diffraction measurements, merit further investigation.

A significant feature detected by electron microscopy is the relatively large number of lattice imperfections in the intercalated complexes, ranging from arrays of edge dislocations and associated stacking faults (Fig. 2, A and B) to vacancies and random alternations of the first-stage with second-stage regions (Fig. 2, C and D), particularly in $TaS_2(C_5H_5N)_{1/4}$. The effect of the lattice imperfections on the physical properties of these new types of highly anisotropic compounds has not yet been examined; however, it is clear that at least some of the lattice imperfections will have to be eliminated or substantially reduced before the intrinsic anisotropy can be realized.

These results demonstrate the unique value of electron microscopy for the

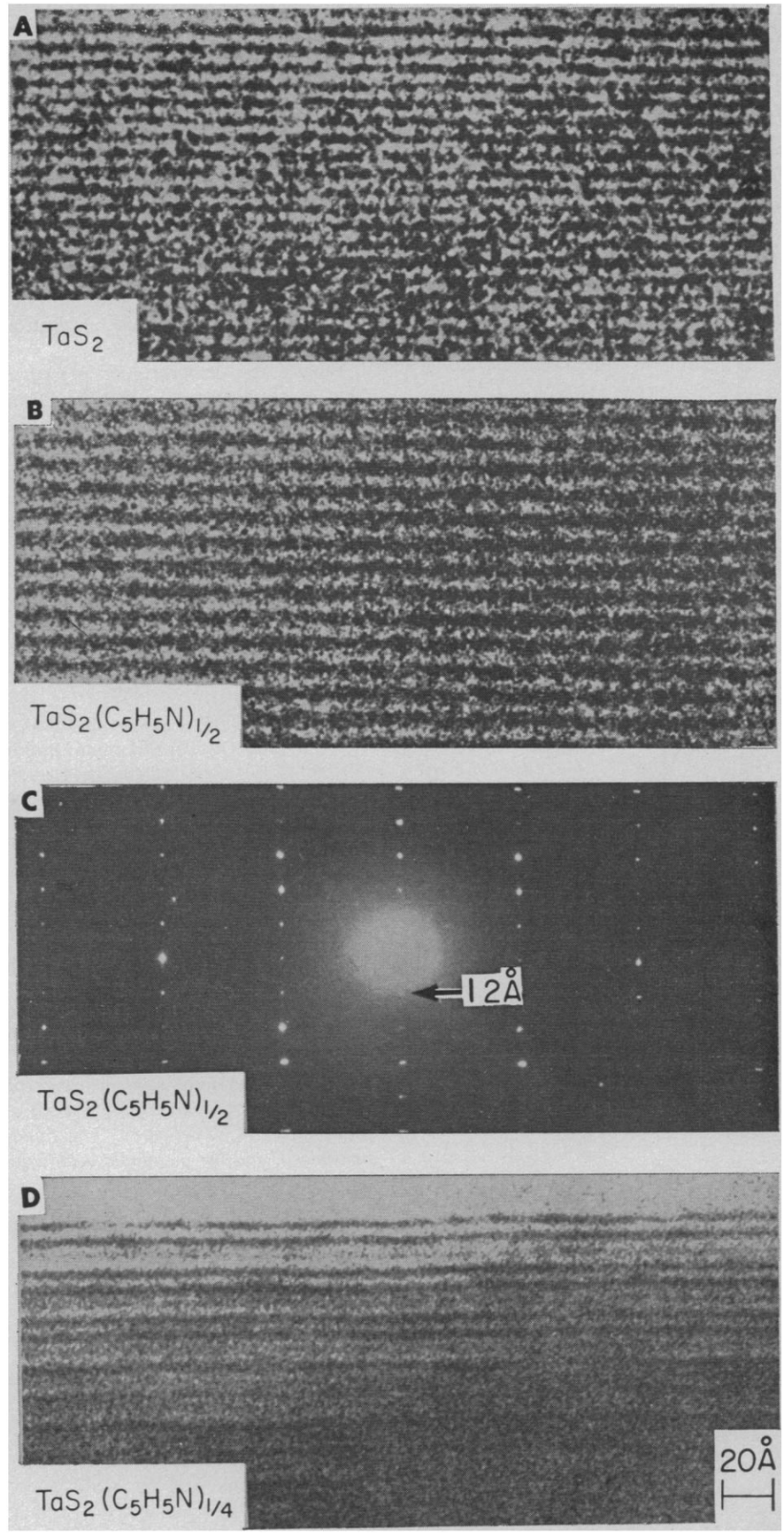

Fig. 1. Electron micrograph (200 kv) showing highly ordered, atomically thin, layered structures in suitably oriented crystals of (A) TaS_2; (B) $TaS_2(C_5H_5N)_{1/2}$; (C) selected-area diffraction pattern with (001) corresponding to the 12-Å layer spacing indicated by the arrow; (D) $TaS_2(C_5H_5N)_{1/4}$. (Magnification, × 3,600,000.)

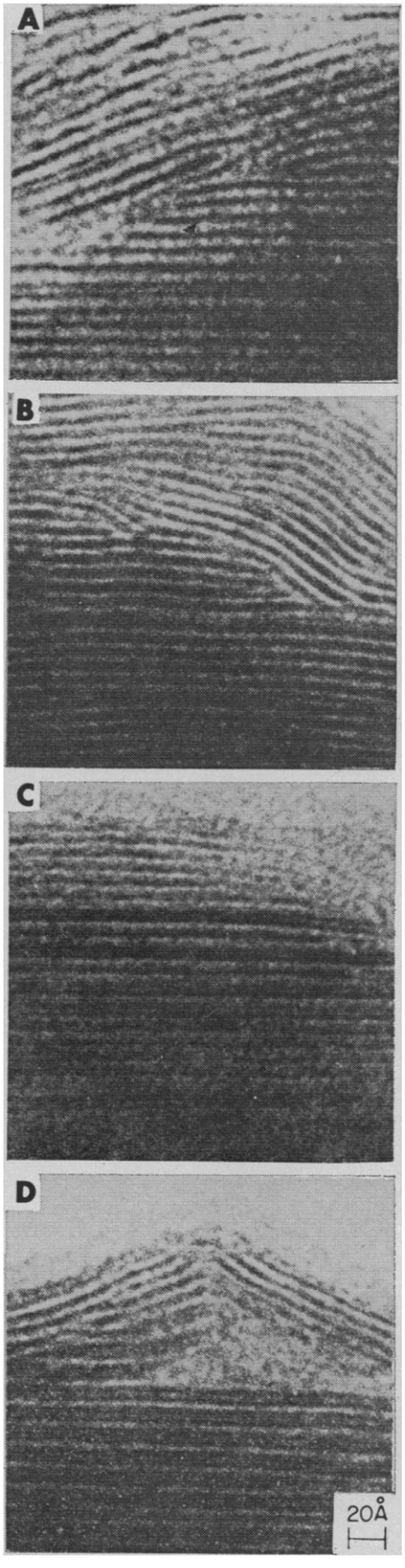

Fig. 2. Dislocations and other crystal lattice imperfections directly resolved by electron microscopy in thin specimens of (A and B) $TaS_2(C_5H_5N)_{1/2}$ showing edge dislocations, associated stacking faults, and first-stage regions alternating with second-stage regions in (C and D) $TaS_2(C_5H_5N)_{1/4}$. (Magnification, × 2,250,000.)

visualization of the structure of the crystalline lattice of layered intercalation compounds down to the atomic level, which can be further extended to the direct study of materials in the superconducting state. Cryo-electron microscopy at liquid-helium temperatures (*6, 10*) may also be used to observe trapped flux patterns by the decoration techniques of Träuble and Essmann (*11*) or through direct visualization of magnetic distribution (*10, 12*) and detection of regular arrays of flux lines in thin films of type II superconductors by electron diffraction (*13*).

Finally, the demonstration presented here of atomically thin metallic layers separated by an organic barrier is also of interest in connection with the general problem of superconducting tunneling (*14*). The multilayered structures of atomic dimensions depicted here are well within the range of tunneling phenomena and might exhibit characteristics related to Josephson tunneling (*15*) in novel ways uniquely derived from the three-dimensional configuration of the layered superconducting intercalation complexes.

H. Fernández-Morán
Mitsuo Ohstuki, Akemi Hibino
Charles Hough
Department of Biophysics, Pritzker School of Medicine, University of Chicago, Chicago, Illinois 60637

References and Notes

1. F. R. Gamble, F. J. DiSalvo, R. A. Klemm, T. H. Geballe, *Science* **168**, 568 (1970).
2. F. R. Gamble, J. H. Osiecki, F. J. DiSalvo, *J. Chem. Phys.*, in press.
3. T. H. Geballe, A. Menth, F. J. DiSalvo, F. R. Gamble, *Phys. Rev. Lett.*, in press.
4. F. R. Gamble, J. H. Osiecki, M. Cais, R. Pisharody, F. J. DiSalvo, T. H. Geballe, *Science* **174**, 493 (1971).
5. H. Fernández-Morán, *Ann. N.Y. Acad. Sci.*, in press; ———, E. F. J. van Bruggen, M. Ohtsuki, *J. Mol. Biol.* **16**, 191 (1966).
6. H. Fernández-Morán, *Proc. Int. Congr. Electron Microsc., 6th* **1**, 13 (1966); *ibid.*, p. 27.
7. ———, M. Ohtsuki, C. Hough, *Proc. Int. Congr. Electron Microsc., 7th* **3**, 9 (1970).
8. J. A. Wilson and A. D. Yoffe, *Advan. Phys.* **18**, 193 (1969).
9. G. A. Bassett, J. W. Menter, D. W. Pashley, *Proc. Roy. Soc. Ser. A Math. Phys. Sci.* **246**, 345 (1958).
10. H. Fernández-Morán, *Proc. Nat. Acad. Sci. U.S.* **56**, 801 (1966); *Proc. Int. Congr. Electron Microsc., 7th* **2**, 91 (1970).
11. H. Träuble and U. Essmann, *J. Appl. Phys.* **39**, 4052 (1968).
12. H. Fernández-Morán, *Exp. Cell Res.* **62**, 90 (1970).
13. ———, M. Ohtsuki, A. Hibino, *Geochim. Cosmochim. Acta*, in press; H. W. Fuller and M. E. Hale, *J. Appl. Phys.* **31**, 238 (1960); M. J. Goringe and J. P. Jakubovics, *Phil. Mag.* **15**, 393 (1967).
14. I. Giaever, *Phys. Rev. Lett.* **5**, 147 (1960).
15. B. D. Josephson, *Advan. Phys.* **14**, 419 (1965).
16. We thank Drs. F. R. Gamble, T. H. Geballe, F. J. DiSalvo, and their colleagues for providing the layered and intercalated transition metal dichalcogenide compounds and for helpful discussions with them and Dr. H. McConnell. We thank J. Richardson, S. Rowe, S. Erikson, C. Weber, G. Bowie, R. Vicario, G. Arcuri, and H. Krebs for valuable assistance. This work has been carried out at the University of Chicago with the support of NIH grant GM 13243, NASA grant 14-001-012, the Pritzker Fund, the L. Block Fund, and the Otho Sprague Memorial Fund of the University of Chicago.

21 July 1971, revised 11 August 1971

Buffer Combinations for Mammalian Cell Culture

Abstract. *The growth and metabolism of cultured mammalian cells are markedly affected by the* p*H variation in ordinary bicarbonate-buffered media (*p*H 8.0 to 6.9). Those* p*H swings can be reduced and the* p*H of the culture can be stabilized as desired in the range* p*H 6.4 to 8.3 by appropriate combinations of two or three organic buffers, each at 10 to 15 millimolar, in conjunction with phosphate and bicarbonate. The initial alkalinization in sparse cultures is then minimized, and the metabolic acidification in 24 hours is usually less than 0.4* p*H unit except in heavy cultures.*

Relatively minor variations in the *p*H of the medium in the range *p*H 6.8 to 8.2 markedly affect the growth of normal, virus-transformed, and cancer cells (*1, 2*). The optimum *p*H varies with the individual strain, from as low as *p*H 6.9 to 7.1 to as high as *p*H 7.6 to 7.8 (*2*). In $NaHCO_3$-buffered media, an initial loss of CO_2 in sparse cultures raises the *p*H to approximately 8.0. This shift is followed by acidification as a result of cell metabolism, with a *p*H after 24 hours as low as 6.9 in heavy cultures. This prolonged exposure to suboptimal *p*H accentuates the sensitivity of normal diploid cells to a growth inhibitory effect of cellular interaction, which develops at relatively low population densities ["contact" inhibition of growth (*3, 4*)]. This population-dependent inhibition can be promoted by appropriate variations in the *p*H of the medium, and can be at close to optimal levels, with a resulting large increase in the maximum population density achieved by normal cells (*2, 5*). Not only the growth of the cells, but other parameters of cellular metabolism may also be affected by *p*H variation (*6*).

The stabilization of *p*H in cell cultures is of some importance. The com-